Molecular Crystals and Liquid Crystals Science and Technology. Section A. Molecular Crystals and Liquid Crystals

Publication details, including instructions for authors and subscription information:
http://www.tandfonline.com/loi/gmcl19

Spin Identification of Polyionic High-Spin Aryl-Based Heteroatomic Systems by 2D Electron Spin Transient Nutation (2D-ESTN) Spectroscopy

Koichi Itoh [a], Shigeaki Nakazawa [b], Masafumi Yano [b], Mutsuo Furuichi [b], Kazunobu Sato [b], Daisuke Shiomi [a], Takamasa Kinoshita [b], Kyo Abe [b] & Takeji Takui [b]

[a] Department of Material Science, Faculty of Science, Osaka City University, Sugimoto, Sumiyoshi-ku, Osaka, 558, Japan

[b] Department of Chemistry, Faculty of Science, Osaka City University, Sugimoto, Sumiyoshi-ku, Osaka, 558, Japan

Version of record first published: 04 Oct 2006

To cite this article: Koichi Itoh, Shigeaki Nakazawa, Masafumi Yano, Mutsuo Furuichi, Kazunobu Sato, Daisuke Shiomi, Takamasa Kinoshita, Kyo Abe & Takeji Takui (1997): Spin Identification of Polyionic High-Spin Aryl-Based Heteroatomic Systems by 2D Electron Spin Transient Nutation (2D-ESTN) Spectroscopy, Molecular Crystals and Liquid Crystals Science and Technology. Section A. Molecular Crystals and Liquid Crystals, 305:1, 515-532

To link to this article: http://dx.doi.org/10.1080/10587259708045085

Mol. Cryst. Liq. Cryst., 1997, Vol. 305, pp. 515–532
Reprints available directly from the publisher
Photocopying permitted by license only

SPIN IDENTIFICATION OF POLYIONIC HIGH-SPIN ARYL-BASED HETEROATOMIC SYSTEMS BY 2D ELECTRON SPIN TRANSIENT NUTATION (2D-ESTN) SPECTROSCOPY

KOICHI ITOH,* SHIGEAKI NAKAZAWA, MASAFUMI YANO, MUTSUO FURUICHI, KAZUNOBU SATO, DAISUKE SHIOMI,* TAKAMASA KINOSHITA, KYO ABE, AND TAKEJI TAKUI
Department of Material Science* and Department of Chemistry, Faculty of Science, Osaka City University, Sugimoto, Sumiyoshi-ku, Osaka 558, Japan

Abstract Molecular design, generation, and spin identification of polyionic high spins with heteroatomic π-conjugation are described. The molecular design was based upon the π-topological pseudo-degeneracy of HOMO's for high-spin polycations and LUMO's for high-spin polyanions. The pseudo-degeneracy originates in heteroatomic perturbation and high spin preference in their ground state is driven by *meta*- or 1,3,5-connectivity of heteroatomic sites giving rise to additive dynamic spin polarization. Polyionic high spins were generated by chemical oxidation or reduction in solution. Thus, the polyions were observed in a rigid glass solution containing reaction mixture. For such complex spin systems their reliable spin identification is essential and, therefore, we employed field-swept 2D electron spin transient nutation (2D-ESTN) spectroscopy. In this work, we have developed such a 2D-ESTN spectroscopy as deserves to enhance spectral resolution in complex spin mixture of non-oriented systems. An unequivocal and facile spin identification of the polyions was carried out, demonstrating that the topological version of the molecular design has been established for polyionic high-spin preference in heteroatomic π-conjugation. It has turned out that the 2D-ESTN spectroscopy is feasible for high spin mixture of any kinds and provides us with direct experimental discrimination between high spins of different spin multiplicities.

INTRODUCTION

Over the last decade, remarkable progress has been made in the field of high-spin chemistry which is the fundamental basis of molecule-based magnetism. Among diverse topics in this field, the high-spin chemistry of charged organic molecules is important in view of new organic materials such as purely organic magnetic metals with both electron conduction and spin alignment.

It has been well established that in the case of neutral high-spin molecules, the spin polarization mechanism dictates their spin alignment as determined by the topology of their π electron networks. Thus the symmetry requirement for the topological degeneracy of the π NBMO de-

termines the spin alignment. In the case of alternant hydrocarbons, the Heisenberg VB picture predicts the number of ground-state spins as the difference between those of the up and down spins which are alternately allocated on carbon atoms in their π electron networks.[1] However, in the case of charged molecules, other competing mechanisms such as charge transfer or spin delocalization mechanism exist, so that their competition determines the final spin alignment.

We have examined the spin alignment in ionized molecular field for organic homoatomic high-spin hydrocarbons,[2-5] and established that if a neutral high-spin system is ionized the resulting ion is also a high-spin system. Therefore, in the case of homoatomic high-spin hydrocarbons, the spin polarization mechanism is so strong that even in a charged molecular field it predominates over spin aligning mechanisms such as spin delocalization.

On the other hand, the spin alignment in organic heteoratomic high-spin molecules with charge has only recently been reported,[6-10] and π topology rule for heteroatomic versions has been examined. It should be emphasized that the π topology rule mentioned above has originally been derived for homoatomic hydrocarbons, and simple analogy is not straightforwardly applicable to heteroatomic high-spin molecules. The π-topology rule is underlain by dynamic spin polarization in π-conjugation network. In this respect, we have recently examined the spin states of polyionic aryl-based heteroatomic high-spin systems in terms of pseudo π-topological degeneracy.

This paper deals with molecular design, generation, and spin identification of polyionic high spins. The molecular design was based upon the pseudo π-topological degeneracy of HOMO's for high spin cations and LUMO's for high spin anions, and polyionic high spins were generated by chemical oxidation or reduction in solution. Thus, the polyions were observed in a rigid glass solution containing reaction mixture. For such complex spin systems their reliable spin identification is essential and, therefore, we employed field-swept 2D electron spin transient nutation (2D-ESTN) spectroscopy. In this work, we have developed such a 2D-ESTN spectroscopy as deserves to enhance spectral resolution in non-oriented high-spin systems.

2D ELECTRON SPIN TRANSIENT NUTATION (2D-ESTN) SPECTROSCOPY

The most conventional method for spin identification is magnetic susceptibility measurements. However, for complex spin systems this method has the disadvantage that it is difficult to measure each component susceptibilities separately because only overall susceptibility could be observed. Conventional cw ESR has better advantage in this respect, but unless we use single

crystals, unequivocal spin identification would also be difficult for mixed spin systems. On the other hand, pulsed ESR especially ESTN is an excellent technique for this purpose and is a powerful tool to distinguish different spin multiplicities.

Isoya *et al.*,[11] and Astashkin and Schweiger[12] have first applied this technique to spectroscopic separation of overlapping ESR spectra as well as identification of electron-spin multiplicities. However, their interests have been directed to paramagnetic species in single crystals which give rather simple spectra. We have for the first time applied this spin identification technique to complex spin systems such as non-oriented multi-spin systems.[13] and developed field-swept 2D-ESTN spectroscopy, which is appreciated for spin mixture of non-oriented systems.

The classical picture of nutational motion may be well understood in the rotating frame x'y'z'. We first consider the motion of spin magnetization in the presence of the static magnetic field as well as the microwave radiation field. When the microwave rotating field $\boldsymbol{B}_1$ with the frequency ω is applied in addition to the external static magnetic field $\boldsymbol{B}_0$, the magnetization vector $\boldsymbol{M}$ precesses around the effective field $\boldsymbol{B}_e$ as shown in Figure 1, where $B_e = [(B_0 - \omega/\gamma)^2 + B_1^2]^{1/2}$ and ω/γ is a fictitious field arising from the rotating frame. This precessional motion is called nutation. The nutation frequency is given by $\omega_n = \gamma B_e$ as the product of magneto-gyric ratio times the effective field. ϕ is the nutation angle made during the pulse length t_1 and is generally given by $\phi = \omega t_1 = \gamma B_e t_1$. On resonance, however, the effective field $\boldsymbol{B}_e$ reduces to the rotating field $\boldsymbol{B}_1$, so the nutation frequency becomes $\omega_n = \omega_1 = \gamma B_1$.

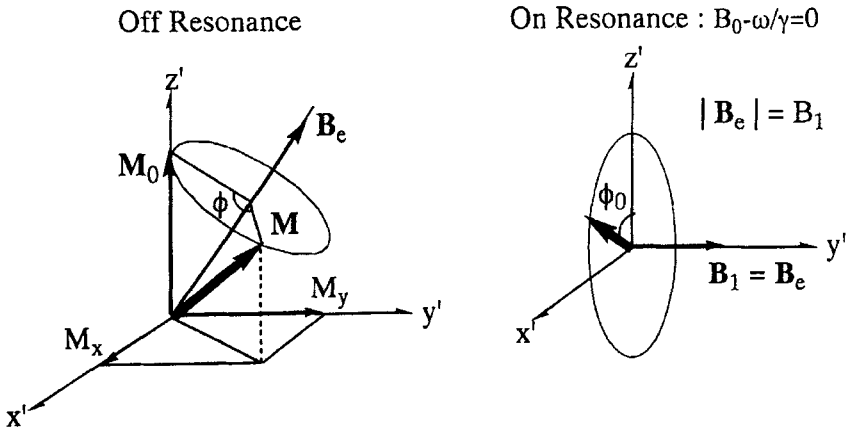

FIGURE 1. Classical vectorial picture for the nutation of the spin magnetization $\boldsymbol{M}$ in the frame rotating with the microwave radiation field $\boldsymbol{B}_1$.

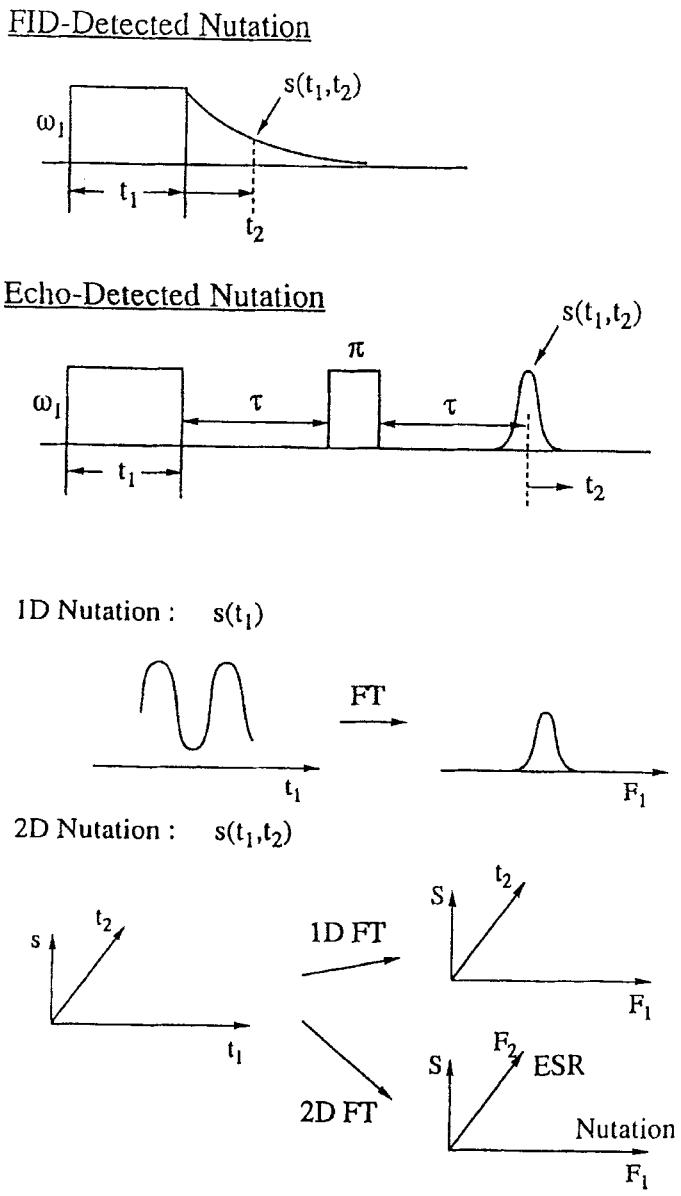

FIGURE 2. Schematic timing diagram for FID- and ESE-detected ESTN experiments, and Fourier transformation of the time domain signal to the frequency domain spectrum.

The nutation spectrum can be detected by means of either FID or electron spin echo (ESE) as a function of the microwave pulse length t_1, and the time t_2 in the time domain as shown in Figure 2. The Fourier transformation of a signal $s(t_1,t_2)$ with respect only to the t_1 axis gives the

one-dimensional (1D) nutation spectrum in the frequency domain. On the other hand, the Fourier transform of $s(t_1, t_2)$ with respect to both the t_1 and t_2 axes gives 2D nutation spectra, where the t_1 and t_2 axes lead to the nutation spectrum and FID- or ESE-detected ESR spectrum in the frequency domain F_1 and F_2, respectively. In fine-structure X-band ESR spectroscopy, a single microwave pulse can not afford to produce the nutation of spin magnetizations on the whole because of the very technical restriction to the strength of the coherent microwave radiation field on the sample site. Fine structure anisotropy usually exceeds the frequency region which is to be covered by the microwave pulse. The situation contrasts with modern NMR spectroscopy. Thus, ESTN spectroscopy in the magnetic field swept mode is required in order to obtain whole nutation spectra from the high spin systems having fine structure terms of spin dipolar interactions. The field-swept mode ESTN spectroscopy is conveniently represented in terms of a two-dimensional (2D) scheme, *i.e.,* $S(F_1, B_0)$ which is Fourier-transformed in the frequency-magnetic field 2D domain. A projection of $S(F_1, B_0)$ on to the B_0 axis gives either an FID-detected or ESE-detected fine-structure ESR spectrum, which corresponds to the conventional cw-ESR spectrum of non-oriented systems under study.

Thus, magnetic field-swept nutation spectra can be obtained in a 2D representation, yielding spectroscopic resolution enhancements and unequivocal *S*-discrimination in the frequency-magnetic field 2D domain . In the field-swept 2D spectroscopy applied to non-oriented systems, all the orientations of the systems more or less contribute to the corresponding nutation frequency spectra at a given resonance field. In order to reconstruct complete nutation-frequency spectra, contributions from the orientations giving rise to the resonance field are evaluated. The field-swept 2D presentation is of essential importance in the ESTN spectroscopy for non-oriented systems, as described below. This novel technique is also applicable to open-shell systems with exchange narrowing lines by the use of an FID detection scheme.[13] In this study, ESTN measurements were made by an ESE detection scheme composed of a three pulse sequence in which an additional $\pi/2$ pulse is applied between the nutation and π pulses as shown in Figure 2, simply because of the occurrence of inhomogeneously broadened cw-ESR lines in organic glasses. The ESTN spectroscopy is essentially free from spectral simulation required for randomly oriented systems in order to identify S and M_S values of high spin systems. In this context, the contrast between the conventional cw ESR and the novel 2D-ESTN spectroscopy is remarkable for randomly oriented or powder-pattern high-spin systems.

In the case of a multi-spin system, each spin experiences dipolar field from other spins in addition to the static and microwave fields. According to a quantum mechanical treatment,[13] the equation of motion for such a spin system can be described in the rotating frame as

$$d|\rho(t)>/d\,t = -\,i[H_0' + H_1(t)']\,|\,\rho(t)> \tag{1}$$

where $H_1(t)' = \omega_1 S_y = \gamma B_1 S_y$ is the perturbing Hamiltonian due to the rotating microwave field, and H_0' is the unperturbed Hamiltonian for the spin system:

$$H_0' = H_{offset} + H_D \tag{2}$$

$$H_{offset} = -\Delta\omega\, S_z \tag{3}$$

$$H_D = \omega_D[S_z^2 - S(S+1)/3] + \omega_E(S_x^2 - S_y^2) \tag{4}$$

H_{offset} represents the Zeeman term in the rotating frame and H_D the fine structure term due to the dipolar field from other spins where ω_D and ω_E are the fine structure parameters in the frequency unit and $\Delta\omega = \omega - \omega_0 = \omega - \gamma B_0$.

The nutation frequency ω_1 is strongly dependent upon the dipolar term H_D relative to the microwave field energy H_1'. However, it reduces to simple expressions for the following two extreme cases:[13]

$$(1)\ H_D >> H_1': \quad \omega_n = \omega_1[S(S+1) - M_S M_S']^{1/2} \tag{5}$$

$$(2)\ H_D << H_1': \quad \omega_n = \omega_1 \tag{6}$$

Case (1) corresponds to the weak perturbation of the microwave field as compared to the dipolar fields from the other spins, and provides us the spin multiplicity of the spin system through Equation (5) where M_S and M_S' denote the electron spin sublevels involved in the allowed ESR transition.[11-13] In case (2), on the other hand, the strong perturbation of the microwave field averages out the dipolar interactions, so that little information can be obtained from the nutation frequency.

For a particular transition $|M_S = +1/2> \Leftrightarrow |M_S = -1/2>$ which is the central transition of a Kramer's doulet with a half-integral spin, the nutation frequency is simply given by

$$\omega_n = (S + 1/2)\omega_1 \quad \text{for} \quad S = 1/2, 3/2, 5/2, \ldots\ldots \tag{7}$$

from Equation (5). On the other hand, for a transition $|M_S = +1> \Leftrightarrow |M_S = 0>$ or $|M_S = 0> \Leftrightarrow |M_S = -1>$ with integral spins, we have

$$\omega_n = [S(S+1)]^{1/2}\omega_1 \quad \text{for} \quad S = 1, 2, 3, \ldots\ldots \tag{8}$$

Thus we can easily draw information about spin multiplicities from observed nutation spectra of complex spin systems if we choose particular transitions described above in the weak extreme limit. For an intermediate case between the two extreme cases (1) and (2), the behavior of the nutation spectrum is rather complicated depending on the ratio ω_D/ω_1. Figure 3 exemplifies the nutation frequency ω_n dependence on ω_D/ω_1 in an ESR transition $|M_S = +1/2> \Leftrightarrow |M_S = -1/2>$ for $S = 3/2$. For the dependence numerical calculation has been carried out on the basis of Liouville-von Neumann equation. For the vanishing ω_D the nutation spectrum is composed of a single frequency component with $\omega_n = \omega_1$. This case is denoted by the arrow (2) on the right in Figure 3. On the other hand, in the weak extreme limit, *i.e.*, $\omega_D/\omega_1 >> 1$, the ratio ω_n/ω_1 is equal to 2 according to Equation (5). This can be seen as indicated by the arrow (1) in Figure 3. Note that the quantitative evaluation of fine structure constants by ESTN spectra is feasible with the help of nutation spectral simulation. Experimentally, this has been demonstrated for Cr^{3+} in MgO powder. It has turned out that the well-known vanishing fine-structure constant for Cr^{3+} in MgO is not correct and the observed non-vanishing D value is due to an appreciable amount of symmetry reduction around the Cr^{3+} site.[13]

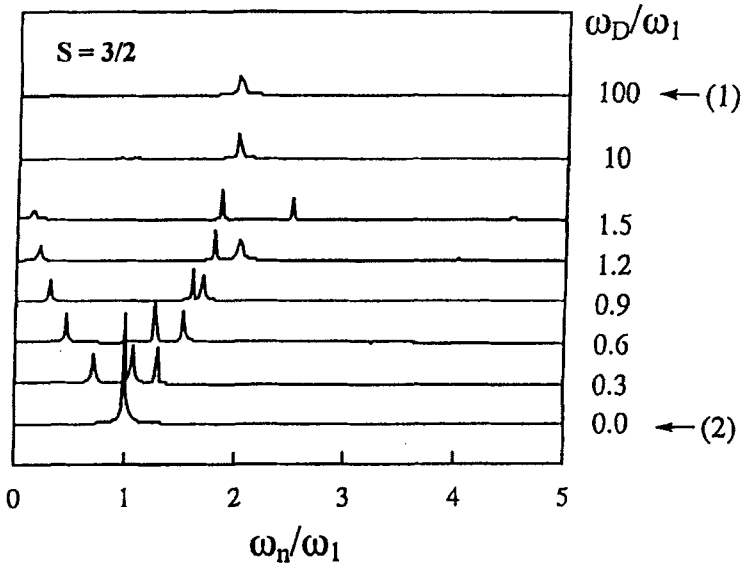

FIGURE 3. Dependence of the nutation frequency ω_n on the ratio ω_D/ω_1 for the allowed ESR transition $M_S = 1/2 \Leftrightarrow M_S = -1/2$ for $S = 3/2$. The arrows (1) and (2) denote the weak extreme limit and the strong extreme limit of the microwave radiation field $B_1 = \omega_1/\gamma$, respectively.

MOLECULAR DESIGN; CRYSTAL ORBITAL APPROACH AND USE OF TOPOLOGICAL PSEUDO-DEGENERACY FOR ORGANIC HIGH-SPINS WITH MULTI-CHARGE

The first documented band-structure calculation,[1a,c] which showed the unlimitedness of the degree of π-topological NBMO degeneracy for 1D neutral ferromagnetic polymers, had appeared at earlier times before crystal orbital approach was established in polymer chemistry. Since then, theoretical studies of the possible occurrence of organic magnetic polymers or extended high-spin systems in terms of band structure calculation have been made in various levels of approximation.[14-23] The model calculation introduced in this section underlying molecular design for magnetic polymers with multi-charge is the simplest possible version for band structure calculations of π-conjugated polymeric systems and their inter-polymer interactions.[23] The extended interpolymer interactions in terms of topological considerations have not been documented. It has been shown that highly topological modulation of electronic band structures gives rise to intriguing spin-polarized magnetic properties of polymeric systems.[23]

The calculation is based on traveling wave (crystal orbital) approach, which corresponds to a description of mobile electrons with non-zero linear momentum in the periodic "lattice" comprised of the N-segment structure of the systems. Translation symmetry requirements are assumed for potential terms and the corresponding Born-von Kármán's periodic boundary condition is also assumed for the total molecular orbital wave function describing the polymeric system under study. The tight binding approximation is used in order to facilitate the calculation by means of Rayleigh-Ritz linear variation method. Electron correlation is not included explicitly. Such improved treatment considering electron correlation has been demonstrated for a simpler segment structure.[23]

Figure 4A and B show the π-crystal orbital band (π-CO band) structure in k wave vector space representation for a neutral extended system of 1D homoatomic π- conjugation and the corresponding one of a precursor extended system of 1D heteroatomic π-conjugation for polycationic high-spin cases, respectively. In the former (A), complete topological N-fold degeneracy in the π-NBCO band at zero energy with N-electron occupancy appears due to the topology of *meta*-connectivity, leading to a ferromagnetic state at 0 K or a superparamagnetic state accommodating N parallel π-electrons. In the latter (B), on the other hand, N-fold topological pseudo-degeneracy in the π-HOCO (highest occupied π-crystal orbital) band which is completely filled with 2N electrons appears just below zero energy in units of -β. The appearance of the both reduced energy and nonzero band width arises from heteroatomic perturbation, notic-

ing that the ABCO (antibonding unoccupied π-crystal orbital) bands undergo much modulation due to the perturbation and considerable departure from the band structure of the homoatomic analog. The topological pseudo-degeneracy in the HOCO band suggests that electron removal by partial or complete oxidation of the precursor generates polycationic high spin multiplets in

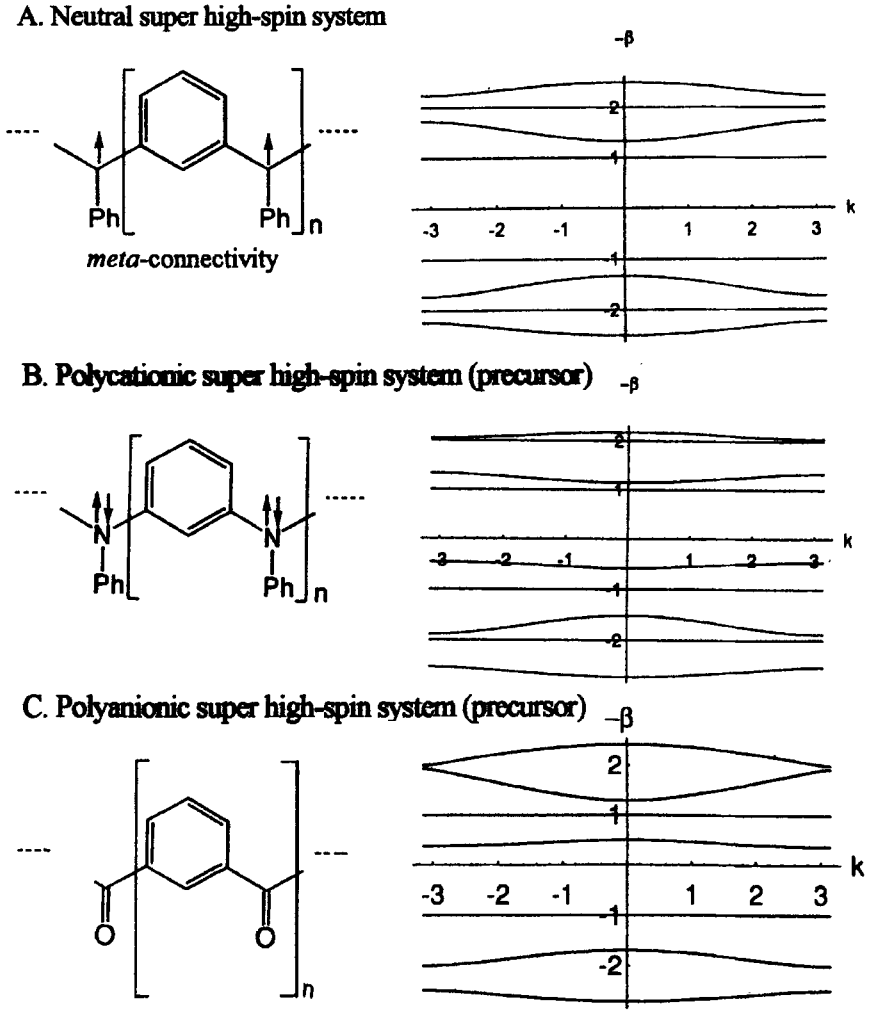

FIGURE 4. π-CO band structures of polymeric high-spin systems of 1D homoatomic π-conjugation (A), and heteroatomic π-conjugation for polycationic case (B) and polyanionic case (C), respectively.

their electronic ground state. This possible occurrence is essentially based on robust dynamic spin polarization taking place in the *meta*-connectivity-based polycationic system, considering the electron repulsion on each carbon sites. The VB description of spin prediction in terms of MO/CO calculations can also give a rationale for the dynamic spin polarization dominating spin alignment in heteroatomic systems,[23] where the spin polarization competes with spin delocalization due to heteroatomic perturbation. The latter favors low-spin ground states. The band width of the HOCO is typically less than 10^{-2} in units of $-\beta$.

In Figure 4C is shown the π-CO band structure for a poly-1,3-ketone precursor of 1D heteroatomic π-conjugation. The topological pseudo-degenerate LUCO (lowest unoccupied CO) band appears close to above zero energy, suggesting the possible occurrence of polyanionic high-spin states by electron doping of the system. Dominant robust dynamic spin polarization is also the case for the occurrence of polyanionic topological high-spin systems under study. Considerably large zerofield splitting parameters, *i.e.*, one order of magnitude larger than those of polycationic cases are anticipated for oligoketone-based intramolecular polyanionic high-spin systems. This is due to the expectation of a considerable contribution from one center n-π spin-spin interaction.

Figure 5 shows star-burst type 2D versions corresponding to those given in Figure 4, depicting complete topological degeneracy appearing at the π-NBCO band (A) for neutral cases and topological pseudo-degeneracies of the π-HOCO band (B) and π-LUCO band (C) near zero energy for polycationic and polyanionic cases, respectively. The band structure in the k wave vector (k_x, k_y) representation reflect the translation symmetry of the systems as well as the topological symmetry. A ferromagnetic or super high-spin ground state is predicted for each 2D polymeric system since the topological 1,3,5-connectivity ensures the occurrence of robust dynamic spin polarization in the open-shell systems under study, *i.e.*, the triaminobenzene-based system for polycationic cases and the tribenzoylbenzene-based system for polyanionic cases. The band width of the HOCO or LUCO band depends highly on both the topology of heteroatomic sites participating in π-conjugation and the Coulomb integral of heteroatoms themselves. Extension of the above approach to 3D polymeric high-spin systems or inter-polymer interactions can be made in order to understand topological nature of 3D electron network or inter-polymer contacts and to serve for molecular design for novel intriguing organic magnetic systems such as interaction-competing molecular systems.

A. Neutral topological high-spin system

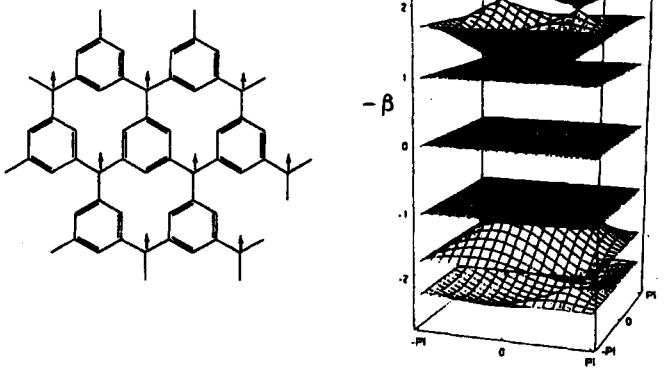

B. Polycationic topological high-spin system

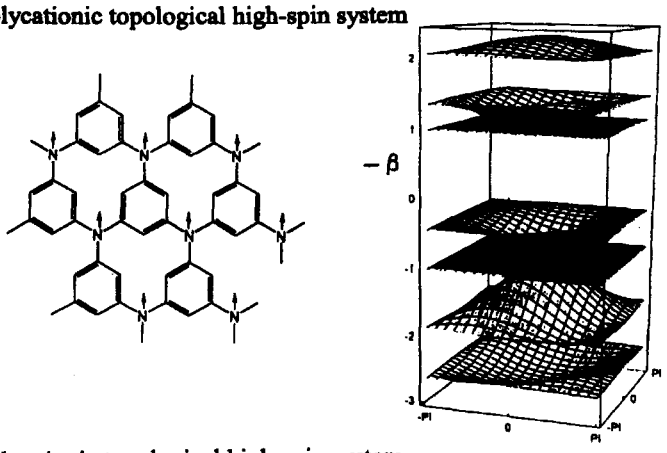

C. Polyanionic topological high-spin system (precursor)

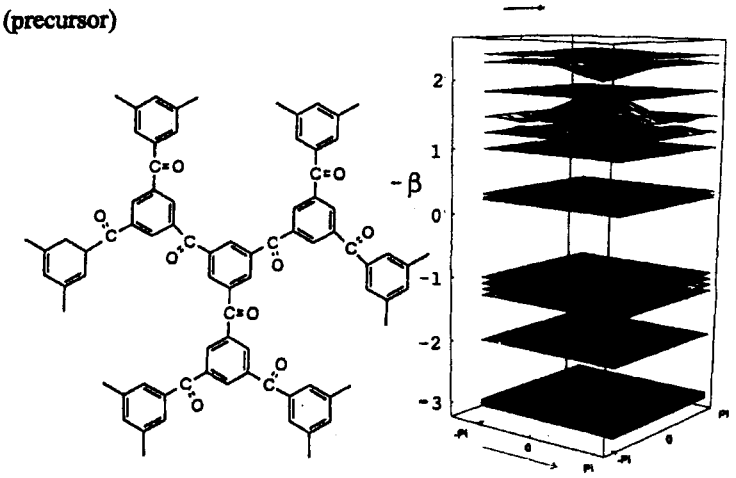

FIGURE 5. Crystal orbital picture in k-vector space for 2D extended systems in the ferromagnetic or super high-spin ground state. (A) Neutral, (B) polycationic, and (C) polyanionic case, respectively.

GENERATION AND SPIN IDENTIFICATION OF HETEROATOMIC HIGH-SPIN POLYIONS

Materials

During the course of model studies of polyionic high-spin oligomers, a series of 1,3-bis(diarylamino)benzenes and 1,3,5-tris(diarylamino)benzenes and their analogues have been adopted for precursors of polycationic high-spin systems. They were synthesized via a sequence of Ullman coupling reactions. 1,3,5-tris(diarylamino)benzenes were synthesized following the reported method. Also, a series of *meta*-, 1,3,5-polyketones and heteroaromatic polyketones have been synthesized for precursors of polyanionic high-spin model oligomers. Their ground-state spin multiplicities of the oxidized or reduced states have been for the first time identified by ESTN spectroscopy applied to randomly oriented high-spin systems in organic rigid glasses. In this paper, only the results of polycationic arylamino-based high-spin systems are described below in order to exemplify the powerfulness of 2D-ESTN spectroscopy applied to non-oriented high-spin sytems.

Generations of the polycationic states of 1 and 2.

Hole doping of neutral diamagnetic molecules can be carried out in an either wet or dry process. The latter involves γ-radiolyses in solids,[2-5] but it does not allow multi-hole doping per molecule under usual conditions. For the multi-hole doping, we adopted a wet process below, *i.e.*, chemical oxidation in solution, which allows multiple-step hole doping and makes cationic molecules undergo the stabilization/relaxation of their molecular structure upon the hole doping in the presence of counter anions.

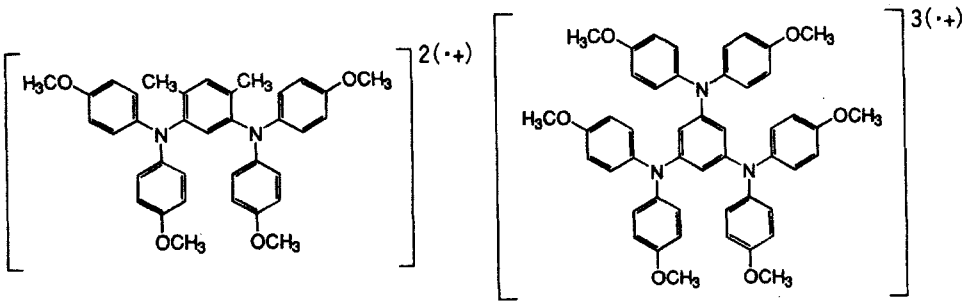

$1^{2(\cdot+)}$ $2^{3(\cdot+)}$

Polycationic state of *N,N,N',N'*-tetra(4-anisyl)-2,4-dimethyl-1,5-phenylenediamine 1. The powder pattern cw-ESR spectrum of the polycationic state of **1** observed at 7 K is shown in Figure 6. There appeared five broad overlapping lines in an allowed ESR transition region. The central intense line suggested the occurrence of $\mathbf{1}^{1(\cdot+)}$ as a doublet species, the overall spectrum not allowing one to characterize the polycationic spin state unequivocally. In order to enhance a spectroscopic resolution with emphasizing S/M_S-discrimination we have measured the ESTN phenomena using the pulsed ESR technique.

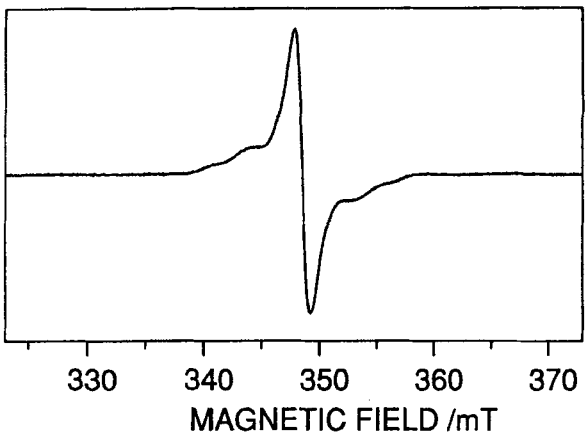

FIGURE 6. Conventional cw-ESR spectrum from the polycationic state of **1** observed at 7 K in dichloromethane.

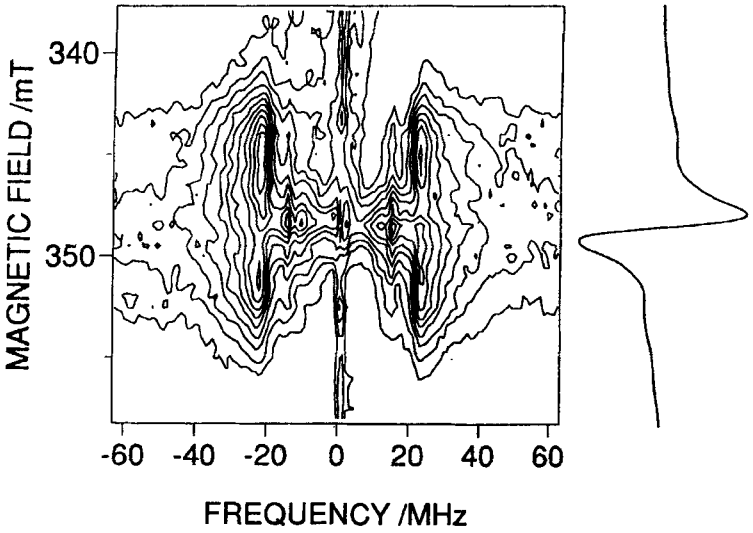

FIGURE 7. Contour plot of the magnetic field swept 2D-ESTN spectra of $\mathbf{1}^{2(\cdot+)}$ and the cw ESR spectrum (on the right) observed at 5 K. ω_I corresponds to nearly 5 MHz.

Figure 7 shows a contour plot of the 2D ESTN spectra of $\mathbf{1}^{2(\cdot+)}$ observed at 5 K. The intense nutation frequency peak observed at 348 mT is seen at 15.3 MHz and both the two peaks at 345 and 351 mT in the wing are seen at 23.1 MHz. The nutation frequency expected for $|1,0\rangle \leftrightarrow |1,\pm1\rangle$ transitions of a triplet state is given by ω_1 from Equation 5. At the central g~2 field region in which both ESR transitions are excited at the same time, the frequency is expected to be ω_1 because of a complete excitation. A frequency ratio of 23.1/15.3 corresponds to that of $\sqrt{2}$ /1 expected for a triplet state from Equation 5. It should be noted that ω_n attributable to a spin doublet is ω_1 because of the vanishing ω_D. The intensity of the peak observed at 348 mT was much stronger than that expected for the triplet state, indicating that signals due to some doublet impurities were overlapping at 348 mT. The powder pattern ESR spectrum, therefore, consists of the signals of the triplet and doublet species which are attributable to the dication of **1** and to the doublet impurities including the monocation of **1**, respectively.

The temperature dependence of the signal intensities was examined in order to determine whether the triplet state of $\mathbf{1}^{2(\cdot+)}$ is a ground or thermally excited state. Since the triplet signals overlap with doublet ones in the observed ESR spectra as shown in Figure 6, we compared the relative intensities of the signals observed at 345.0 mT (central peak) and 341.0 mT in the wing. The temperature dependence of the triplet signal depended linearly with that of the central peak that dominantly consisted of doublet impurities. It was therefore concluded that the dicationic state of **1** is a ground-state triplet.

For the triplet state of $\mathbf{1}^{2(\cdot+)}$, the fine-structure parameter $|D|$ was determined to be 0.007 cm^{-1} from a splitting between the Z transitions in the ESR spectrum. Determination of the E value was erroneous because of low spectral resolution. The $|D|$ value is close to those (0.0064 ~ 0.0079 cm^{-1}) of neutral high-spin molecules with the similar electronic spin structure which have been reported so far, [24-27] suggesting that the π-π two-center spin-spin interactions and dynamic spin polarization dominate the spin alignment and that judging from the $|D|$ values charge fluctuation does not apparently affect the spin polarization mechanism.

The magnitude of the D value of $\mathbf{1}^{2(\cdot+)}$ is consistent with that of $\mathbf{2}^{3(\cdot+)}$ if the projection factor $2S$ - 1 for D values is considered. The comparison is based on order-of-magnitude estimation. Nevertheless it indicates that the similar values of $(2S - 1)|D|$ between $\mathbf{1}^{2(\cdot+)}$ and $\mathbf{2}^{3(\cdot+)}$ are due to the similarity of their spin structures. In this context, detection and identification of $\mathbf{2}^{2(\cdot+)}$ is interesting to understand the molecular structures vs. charge fluctuations of these cationic states with counter anions.

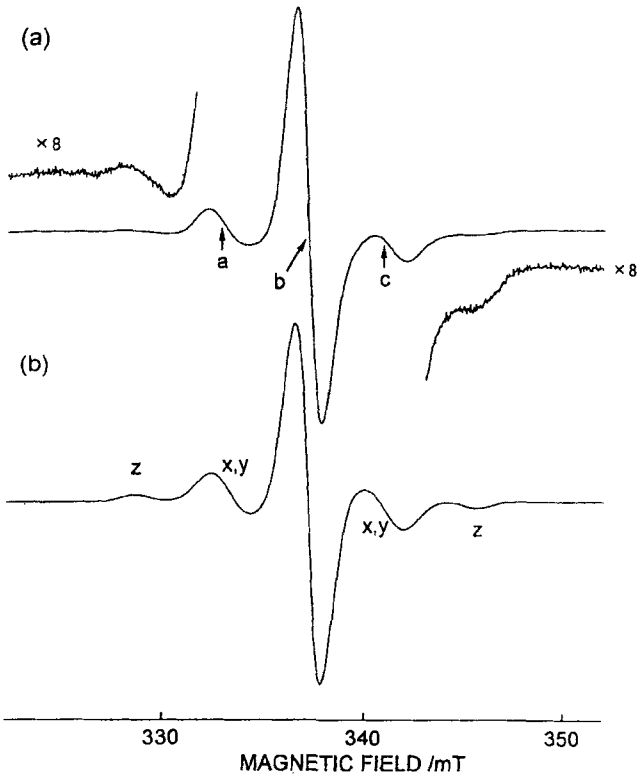

FIGURE 8. Fine-structure cw ESR spectrum of $\mathbf{2}^{3(\cdot+)}$. (a) Observed at 7 K. Microwave frequency was 9.44751 GHz. (b) Simulated with $S = 3/2$, g = 2.0023, $|D| = 0.004$ cm^{-1}, and $|E| = 0.0002$ cm^{-1}.

Tricationic state of *N, N, N', N', N'', N''*-hexa (4-anisyl)-1, 3, 5-triamonobenzene 2.

Figure 8(a) shows the cw ESR spectrum of a tricationic state of **2** observed at 7 K in a dichloromethane glass. The five broad lines were assigned to canonical peaks apparently chacteristic of the allowed ESR transitions from the quartet state with $|D| = 0.004$ cm^{-1}, $|E| = 0.0002$ cm^{-1}, and g = 2.0023 (isotropic). The simulation spectrum is shown in Figure 8(b), from which the hyperfine constants for three nitrogen and proton nuclei were derived. In order to identify the molecular spin multiplicity of the cationic state of **2**, we carried out the ESTN measurements. Figure 9 shows a contour plot of 2D-ESTN spectra of $\mathbf{2}^{3(\cdot+)}$ observed at 6 K in the dichloromethane glass. The intense nutation frequency peak observed at 336.8 mT appears at 10.08 MHz, and both the two peaks at 333.0 and 340.4 mT appear at 8.12 MHz. A ratio of the observed nutation frequencies, 10.08/8.12, agrees with that of $2/\sqrt{3}$ to be expected for a quartet spin state from Equation (5). Thus, unquivocal assignments are as follows: the intense peak

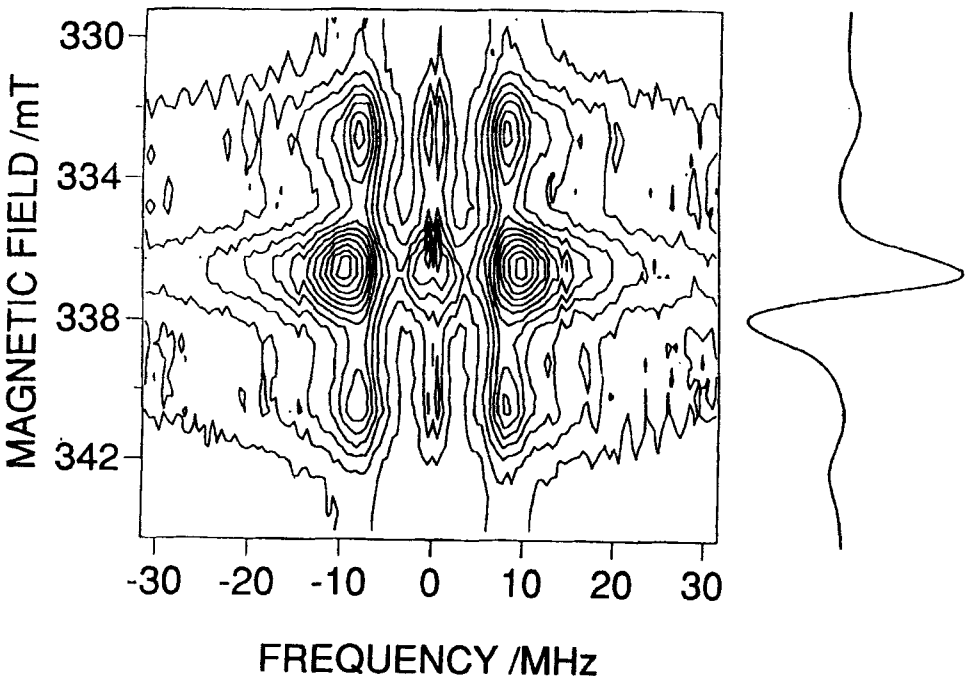

FIGURE 9. Contour plot of the field swept 2D-ESTN spectra of $2^{3(\cdot,+)}$ and the conventional field-swept cw ESR spectrum (on the right) observed at 6 K. ω_I corresponds to nearly 5 MHz.

corresponds to the $|\ S = 3/2, M_s = 1/2\rangle \Leftrightarrow |\ S = 3/2, M_s = -1/2\rangle$ transition and the two weak peaks to the $|\ S = 3/2, \pm 3/2\rangle \Leftrightarrow |\ S = 3/2, \pm 1/2\rangle$ transitions of a pure quartet state. In the 2D-ESTN representation any peaks are not seen at 5 MHz (ω_I) which corresponds to the $S = 1/2$ nutation frequency. This straightforwardly shows that the quartet state is a ground state. If the quartet state is an excited state, the frequency component ω_I arising from a doublet ground state has to be observed. If the energy gap between the doublet and quartet state was comparable with 0.3 cm^{-1}, the effects of spin quantum mixing would appear in the fine-structure spectra. The mixed-doublet peak from organic species is predicted to appear at the $g \sim 2$ field region with a reduced intensity. The 2D-ESTN experiments in the wide range of temperature indicated that an excited doublet state can be located higher than 100 cm^{-1} above the quartet ground state.

CONCLUSION

Polycationic high-spin molecules with heteroatomic π-conjugation network were generated by chemical oxidation and the spin multiplicities in their ground state were unequivocally identified by magnetic field swept 2D-ESTN spectroscopy for non-oriented high-spin systems. The molecular design was based upon the π-topological pseudo-degeneracy of HOMO's for the polycationic high-spin molecules. The present approach is a topological version of the molecular design for polyionic high-spin preference in heteroatomic π-conjugation. The pseudo-degeneracy originates in heteroatomic perturbation. It is concluded that the high spin preference in their ground state is driven by *meta*- and 1, 3, 5-connectivity of heteroatomic sites giving rise to robust and additive dynamic spin polarization. The model system $\mathbf{1}^{2(\cdot+)}$ is the first prototypical example for one-dimensional high-spin polycations. Also, it is shown that the 2D-ESTN spectroscopy is feasible for the spin identification of high spin mixtures of any kinds and provides us with direct and facile experimental discrimination between high spins of different spin multiplicities.

ACNOWLEDGMENTS

This work has been partially supported by Grants-in-Aid for Scientific Research on Priority Areas "Molecular Magnetism" (Area No. 228/04 242 103 and 04 242 105) and Grants-in-Aid for Encouragement of Young Scientists (K. S. and D. S.) from the Ministry of Education, Science and Culture, Japan and also by the Ministry of International Trade and Industries (NEDO project "Organic Magnets").

REFERENCES

1. A. A. Ovchinnikov, *Theor. Chim. Acta,* **47**, 259 (1978); D. J. Klein, C. J. Nelin, S. Alexander, and F. A. Matsen, *J. Chem. Phys.* **77** 3101 (1982); Y. Teki, T. Takui, M. Kitano, and K. Itoh, *Chem. Phys. Lett.,* **142**, 181 (1987).
2. M. Matsushita, T. Momose, T. Shida, Y. Teki, T. Takui, K. Itoh, *J. Am. Chem. SoC.,* **112**, 4700 (1990).
3. M. Matsushita, T. Nakamura, T. Momose, T. Shida, Y. Teki, T. Takui, T. Kinoshita and K. Itoh, *J. Am. Chem. Soc.,* **114**, 7470 (1992).
4. M. Matsushita, T. Nakamura, T. Momo se, T. Shida, Y. Teki, T. Takui, T. Kinoshita, and K. Itoh, *Bull. Chem. Soc. Japan.,* **66**, 1333 (1993).
5. T. Nakamura, T. Momose, T. Shida, T. Kinoshita, T. Takui, Y. Teki, and K. Itoh, *J. Am. Chem. Soc.,* **117**, 11292 (1995).

6. K. R. Stickley and S. Blackstock, *J. Am. Chem. Soc.*, **116**, 11576 (1994).
7. M. Celina, R. L. R. Lazana, M. Luisa, T. M. B. Franco, M. Candida, and B. L. Shohoji, *J. Chem. Research(S)*, 48 (1996).
8. K. Okada, T. Imakura, M. Oda, H. Murai, and M. baumgarten, *J. Am. Chem. Soc.*, **118**, 3047 (1996).
9. A. P. West, Jr., S. K. Silverman, and D. A. Dougherty, *J. Am. Chem. Soc.*, **118**, 1452 (1996).
10. T. Nakamura, T. Momose, T. Shida, K. Sato, S. Nakazawa, T. Kinoshita, T. Takui, K. Itoh, T. Okuno, A. Izuoka, and T. Sugawara, *J. Am. Chem. Soc.*, **118**, 8684 (1996).
11. J. Isoya, H. Kanda, J. R. Norris, J. Tang, M. K. Rowman, *Phys. Rev.*, **B41**, 3905 (1990).
12. A. V. Astashkin and Schweiger, *Chem. Phys. Lett.*, **174**, 595 (1990).
13. K. Sato, K. Shiomi, T. Takui, and K. Itoh, *J. Spectrosc. Soc. Japan*, **43**, 280 (1994).
14. (a) K. Yamaguchi, Y. Toyoda, and T. Fueno, *Chemistry*, **41**, 585 (1986). (b) K. Yamaguchi, Y. Toyoda, and T. Fueno, *Synth. Met.*, **19**, 81 (1987). (c) K. Yamaguchi, Y. Takahara, T. Fueno, K. Nakatsuji, and I. Murata, *Japan J. Appl. Phys.*, **27**, L766 (4987). (d) K. Yamaguchi, H. Namimoto, T. Fueno, T. Nogami, and T. Shirota, *Chem. Phys. Letters*, **166**, 408 (1990). (e) K. Yamaguchi, *Int. J. Quantum Chem.*, **37**, 167 (1990) and references therein.
15. K. Yamaguchi, M. Okumura, J. Maki, and T. Noro, *Chem. Phys. Letters*, **207**, 9 (1993).
16. S. Yamanaka, T. Kawakami, M. Okumura, and K. Yamaguchi, *Chem. Phys. Letters*, **233**, 257 (1995) and references therein.
17. (a) A. Ikawa, H. Mizouchi, and H. Fukutome, *Mol. Crys. Liq. Cryst.*, **271**, 155 (1995) and references therein. (b) H. Mizouchi, A. Ikawa, and H. Fukutome, *Synth. Met.*, **85** (1997).
18. (a) N. Tyutyulkov, P. Schuster, and O. E. Polansky, *Theor. Chim. Acta*, **63**, 291 (1983). (b) N. Tyutyulkov, O. E. Polansky, P. Schuster, S. Karabunarliev, and C. I. Ivanov, *Theor. Chim. Acta*, **67**, 211 (1985).
19. K. Nasu, *Phys. Rev.*, **33B**, 330 (1986).
20. T. Hughbanks and M. Ketesz, *Mol. Cryst. Liq. Cryst.*, **176**, 115 (1989).
21. K. Yoshizawa, A. Tanaka, K. Tanaka, and T. Yamabe, *Poly. J.*, **24**, 857 (1992).
22. A. Mishima, *Mol. Cryst. Liq. Cryst.*, **233**, 61 (1993) and references therein.
23. T. Takui, Y. Teki, K. Sato, and K. Itoh, *Mol. Cryst. Liq. Cryst.*, **272**, 1 (1995).
24. (a) A. Rajca, S. Utamapanya, and J. Xu, *J. Am. Chem. Soc.*, **113**, 9235 (1991). (b) A. Rajca, *Chem. Rev.*, **94**, 871 (1994) and references therein. (c) A. Rajca, and S. Rajca, *J. Am. Chem. Soc.*, **117**, 9172 (1995).
25. G. R. Luckhurst, G. F. Pedulli, and M. Tiecco, *J. Chem. Soc. B*, 329 (1971).
26. G. Kothe, K.-H. Denkel, and W. Sümmermann, *Angew. Chem. Int. Ed. Engl.*, **9**, 906 (1970).
27. J. Veciana, C. Rovira, M. I. Crespo, O. Armet, V. M. Domingo, and F. Palacio, *J. Am. Chem. Soc.*, **113**, 2552 (1991).